Direct Access to Subsurface Sites in Gas-Surface O_2/Ag(210) Interactions using Supersonic Molecular Beams

L. Vattuone, L. Savio,* and M. Rocca

IMEM-CNR, Sezione di Genova and INFM, Dipartimento di Fisica, Università di Genova, Via Dodecaneso 33, 16146 Genova, Italy

(Received 9 October 2002; published 6 June 2003)

We show with supersonic molecular beams and surface vibrational spectroscopy that, contrary to the case of Ag(100) and Ag(110), O_2 undergoes total dissociation on Ag(210) at 105 K. Moreover, metastable subsurface sites can be accessed either directly or indirectly. For the direct channel, the final configuration of the oxygen atoms depends on the angle and the energy with which the gas-phase molecules collide with the surface, being largest for normal incidence on the (100) nanofacets. Access into the subsurface site is enabled only in the presence of preadsorbed oxygen adatoms.

DOI: 10.1103/PhysRevLett.90.228302 PACS numbers: 82.20.–w, 79.20.Uv, 82.30.Fi, 82.65.+r

At the nanoscopic level, the selectivity of chemical reactions is determined by the branching ratio among the different reaction channels leading to the formation of different products. For heterogeneous phase reactions following the Langmuir-Hinshelwood mechanism, the chemical process can be divided into a first step, in which the gas-phase molecules stick at the surface and diffuse to the stable adsorption sites, and a second step, in which the coadsorbed species react [1]. These steps may be limited by kinetic constraints as well as by the presence of potentially active sites, possibly at defects, and by their activation by coadsorbates or by subsurface species, an effect known as "structure gap." Together with the pressure gap, it makes the idealized reaction conditions studied in ultrahigh vacuum different from the real conditions present in industrial reactors. Overcoming these gaps is therefore mandatory for the understanding of heterogeneous phase chemistry at the nanoscopic level. In particular, the detailed mechanisms governing the access to subsurface sites are still not known in detail, due to the difficulty in monitoring these species with usual surface science techniques. Ethylene epoxidation, a reaction at the basis of a billion dollar industry and for which Ag powders show a unique and thus far not understood selectivity [2,3], became a paradigm for reactions influenced by defect sites and possibly by subsurface oxygen [4]. To the best of our knowledge, this is the first time that a subsurface site is populated in a controlled way.

We show here that, for the O_2/Ag(210) system, the final configuration of the adsorbate is very different from the one observed on extended terraces: Open steps induce total dissociation also at temperatures at which only molecular chemisorption occurs on Ag(110) and Ag(100) [5–7]. Moreover, preadsorbed oxygen opens efficient pathways leading, either directly or indirectly, to the occupation of metastable subsurface sites. The absorption process is strongly anisotropic, depending on energy and angle of incidence of the incoming molecules.

The interaction of O_2 with flat and defected Ag single crystal surfaces has been studied thoroughly in our laboratory. In particular, we demonstrated that, at crystal temperatures $T < 150$ K, only molecular adsorption occurs on Ag(110) and Ag(100), while partial dissociation takes place for defected Ag(100) [8] and for Ag(410) [9]. At higher temperatures, dissociation occurs on Ag(110) [10] while desorption dominates on Ag(100) [11]. On Ag(100), oxygen dissociation takes place mainly at open defect sites such as kinks at closed packed steps or open steps running along [100] directions [8,12]. In this process, some oxygen atoms end up in subsurface sites [13]. Subsurface species may be either the only reactive species [14] or affect significantly the reactivity of surface species, as suggested by many investigations trying to unravel the unique selectivity of oxygen for the ethylene epoxidation reaction [4,15]. We demonstrated recently that subsurface oxygen can stabilize CO adsorption on Ag(001) at temperatures (100 K and above) at which no stable CO adsorption occurs on a clean surface [16].

The geometry of the (210) surface and the different surface and subsurface sites for oxygen adatoms are reported in the inset of Fig. 1. The surface is built by (110) and (100) nanofacets, as previously investigated Ag(410) [9], but the (100) terraces consist of one single atomic row and host only half a (100) unit cell. The step edges have an open geometry and run along ⟨100⟩. The normal to the nanofacets is 18.5° and −26.5° off the surface normal for (110) and (100), respectively. The crystal is a 7 mm disk aligned within 0.1° with the (210) plane. Its surface was prepared in ultrahigh vacuum by sputtering and annealing to 700 K. Surface cleanliness was checked by high resolution electron energy loss spectroscopy (HREELS); surface order and azimuthal orientation were controlled by inspection of low energy electron diffraction. The experiments were performed with a coupled supersonic molecular beam plus HREELS system [17] which allows dosing the gas-phase molecules at well-defined angles of

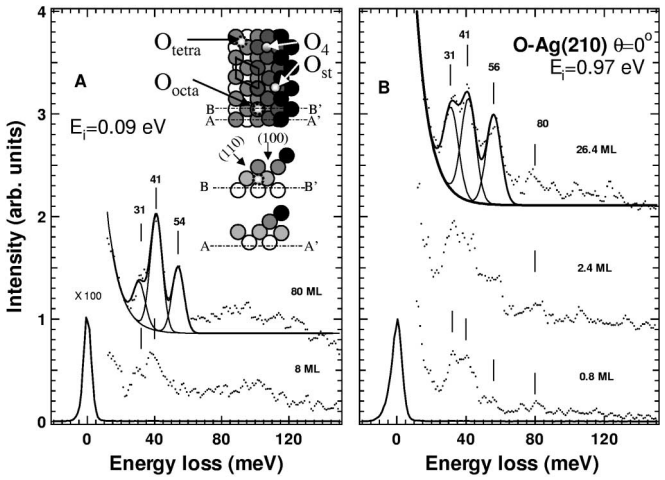

FIG. 1. HREEL spectra recorded after different O_2 exposures at $\theta = 0°$ and $T = 105$ K. Panel (A): $E_i = 0.09$ eV; Panel (B): $E_i = 0.97$ eV. The low energy losses are due to different atomic oxygen moieties; the continuous line is a best fit to the data resulting from the superposition of three components (also shown). The little intensity at 80 meV is due to traces of O_2, presumably adsorbed at extended (110) nanofacets resulting from defects of the (210) geometry. The (210) geometry and the different possible surface and subsurface sites are shown in the inset.

incidence, θ (angular divergence of the beam 0.25°), and translational energy, E_i [full width at half maximum of the energy distribution $(\Delta E_i)/E_i = 0.2$]. The beam energy can be controlled by varying the nozzle temperature and by seeding O_2 in He (3% O_2 in He). The final adsorption state is monitored by HREELS. The electron energy was set to ≈ 2 eV for most measurements and the scattering angle to $\theta_e = 63°$. The energy resolution of the electron beam read typically between 6 and 7 meV. The scattering plane was aligned in the $\langle 1\bar{2}0 \rangle$ direction across the surface trenches.

In Fig. 1, we show HREEL spectra recorded after exposing Ag(210) at $T = 105$ K to O_2 doses performed with $\theta = 0°$ and two different E_i. We notice that (i) the O_2 dose needed to reach a given coverage (i.e., a given intensity of the loss peaks) depends on E_i being larger at low E_i. The adsorption process is therefore globally activated. (ii) Little or no signal is present in the spectral region of the internal O_2 stretch (79–85 meV region), indicating that adsorption is purely dissociative already at 105 K, contrary to the case of low Miller index surfaces and of Ag(410). The (100) nanoterraces are therefore too small to stabilize admolecules. (iii) Three moieties of oxygen form in the dissociation process, vibrating at $\hbar\omega \approx 31$, 40, and 56 meV, respectively. The ratio of the intensity of these losses depends on coverage, E_i, θ, and T, excluding that these modes might be parallel vibrations of a single adsorbate moiety. In the initial stages of the adsorption process, only the losses at 31 and 40 meV are present (see lowest spectra in Fig. 1). These frequencies, observed also for O/Ag(410) [9], are close to those reported for O/Ag(100) and O/Ag(110), respectively. We therefore assign them to oxygen atoms sitting at the (100) nanofacets (O_4) and to Ag-O chains (O_{st}) at the step edges. The relative intensity of the 31 meV loss is smaller when O_2 is dosed at lower E_i. The activation barrier for this pathway is therefore larger than for the formation of the 40 meV moiety only. These observations are in accord with that previously reported for O_2/Ag(410) [9].

The relative weight of the loss at 56 meV grows with O_2 exposure. The assignment of this peak is more problematic since its frequency, never reported for O/Ag, is abnormally high for oxygen adatoms and abnormally low for O_2 admolecules. The latter species is excluded because we observe no O_2 desorption when heating the crystal to temperatures at which the loss disappears and, more importantly, because of the behavior of the 56 meV loss as a function of T. As shown in Fig. 2(A), when T increases the losses at 40 and at 56 meV become initially sharper and grow in intensity (the latter shifting to 58 meV), while the loss at 31 meV disappears. The 58 meV species can therefore be populated by adatoms overcoming thermally an activation barrier of ≈ 0.3 eV (assuming a prefactor of 10^{12} Hz), a process which cannot lead to admolecules. This site does not correspond, however, to an absolute minimum of the free energy since the loss disappears for $T > 300$ K. The 40 meV loss shifts then to 38 meV and broadens considerably, indicating that the oxygen layer has disordered. Room temperature coincides with the onset of oxygen mobility towards deeper bulk sites [12], such as octahedral interstitials O_{octa}, in which it cannot be any more directly monitored by HREELS. The broadening could be connected to the

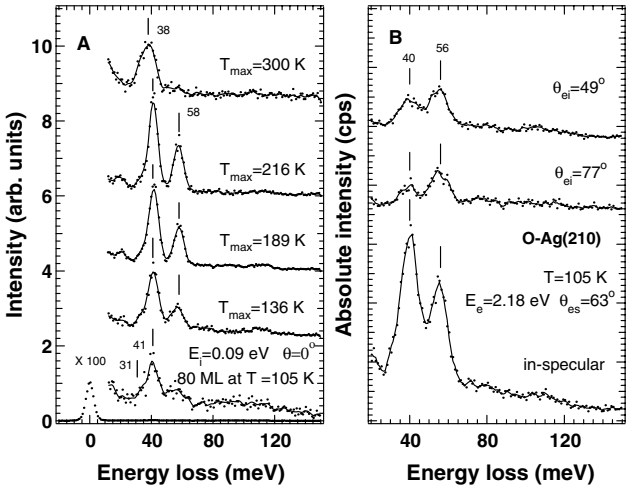

FIG. 2. Panel (A): HREEL spectra recorded in-specular, after dosing O_2 at $T = 105$ K and after flashing the crystal to T_{max}. Panel (B): Non-normalized HREEL spectra recorded in- and out-of-specular for a surface covered with the 40 and 56 meV moieties. The continuous line is the result of a smoothing procedure.

relative position of subsurface oxygen and adatoms. The remaining adatoms desorb at ≈ 470 K. $\hbar\omega = 56$ meV is plausible for oxygen in subsurface sites, since it is larger than for adatoms by roughly a factor of $\sqrt{2}$, i.e., by the ratio expected if the number of Ag-O bonds in the vertical direction doubles and the force constants are not too strongly modified. In accord with this assignment, the 56 meV loss has a strong impact scattering component as witnessed by the measurements reported in Fig. 2(B): Off-specular, the ratio between the loss intensities at 40 and 56 meV is inverted. Similar arguments were often used to assign loss peaks to subsurface species [18–20].

In Fig. 3, we show HREEL spectra recorded after dosing O_2 for different angles and for three E_i. The data were recorded for exposures, χ, corresponding to an intermediate O coverage. χ is different for the different E_i in order to achieve a comparable coverage for all experiments. As it is apparent, the intensity of the losses depends on θ and E_i. In particular, it is nearly isotropic for the highest energy loss at low E_i, but strongly peaked around the normal to (100) nanofacets at large E_i. For $E_i = 0.97$ eV, the access probability into this site is nearly twice as large as for $\theta = -35°$. Little happens in these conditions to the initial sticking coefficient (not shown), in accord with the above-mentioned fact that the 56 meV moiety is populated only in the presence of preadsorbed O. The loss intensities of the spectra of Fig. 3, determined by fitting the experimental curves with three Gaussians and a background consisting of an exponential plus a constant, are reported vs θ and parametric in E_i in Fig. 4. To correct for the slightly different coverage achieved in the experiments, we plot the ratio of the inelastic current in a given channel, I_ω, normalized to the total inelastic current $I_{\text{tot}} = I_{31} + I_{40} + I_{56}$. This procedure allows for a direct comparison of the different relative abundance of each species. The overall dependence on θ is unaffected by this treatment as demonstrated by the curves corresponding to different exposures with $E_i = 0.09$ eV. As one can see in Fig. 4, I_{40}/I_{tot} is nearly independent of θ while I_{31} and I_{56} are strongly angle dependent and at high E_i show a narrow minimum and maximum around $\theta = -26°$, respectively.

The extra channel for accessing the subsurface sites exists only in the presence of preadsorbed oxygen adatoms. However, since I_{56} is nonzero also for positive θ, an alternative pathway leading to the subsurface site must exist, which implies a molecular precursor sufficiently long-lived and mobile to allow searching for the active site. We notice that the final state reached for $E_i = 0.09$ eV (precursor mediated adsorption only, $\hbar\omega = 53$ meV) and for larger E_i ($\hbar\omega = 56$ meV) is different, the frequency shift being small but outside of experimental error. Since the loss frequency increases to 58 meV when annealing the crystal (see Fig. 2), we suggest that the extra energy available at large E_i is used to relax the Ag atoms around the subsurface oxygen. This observation implies that for the directional channel incorporation occurs directly. We exclude incorporation of O atoms to occur via collision of the incoming O_2 molecules with preadsorbed O since the cross section required to justify the observed intensities of the 56 meV vibration would be of the order of several Å^2, i.e., more than 100 times larger than reported for other collision induced processes with comparable activation barrier, as, e.g., O_2/Ag(100) [21]. Moreover, the weight of the 56 meV loss would be expected to increase significantly from $E_i = 0.39$ eV (energy transfer just above threshold) to 0.97 eV, contrary to experimental evidence.

The metastable subsurface site needs to be sufficiently close to the surface to allow for the dipolar excitation of the oxygen vibration with electrons, since not all intensity in Fig. 2(B) is due to impact scattering. The tetrahedral

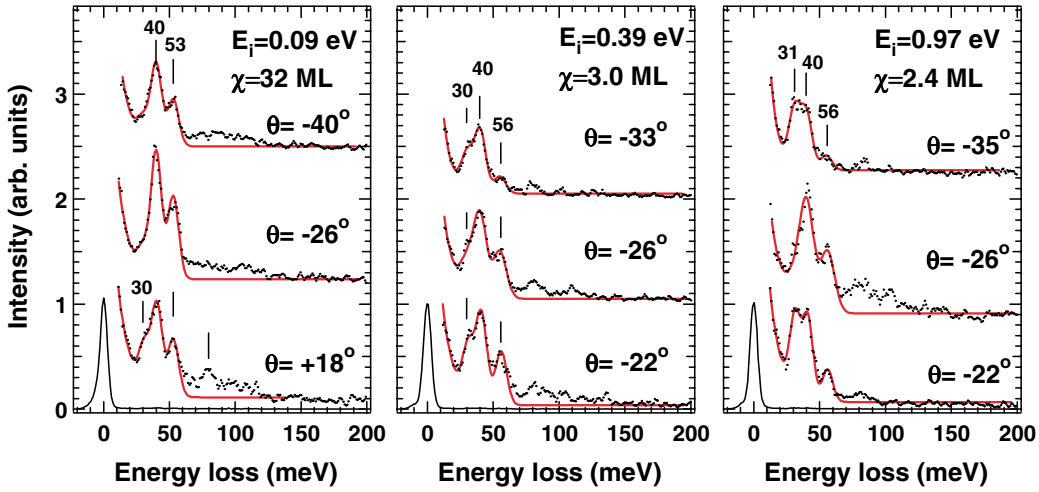

FIG. 3 (color online). HREEL spectra recorded after dosing O_2 at $T = 105$ K with different E_i and θ. The continuous line is a best fit to the data.

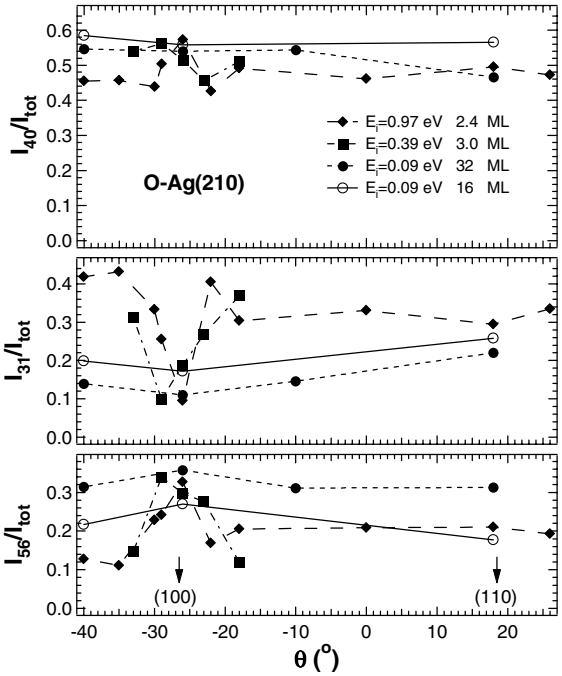

FIG. 4. From top to bottom: I_ω vs θ and parametric in E_i. The data for $E_i = 0.09$ eV are reported for two different χ to show that, although I_{56} is larger at larger χ, the overall angular dependence is not affected.

interstitial O_{tetra} is better suited for this than O_{octa}, since the former is located immediately below the bridge between neighboring atoms of the (100) nanofacets while the latter is right below the Ag atoms at the step edge. Access to it from the vertical direction could reasonably take place only along particular trajectories and be facilitated by an expansion of the lattice at the step edge. A recent *ab initio* theoretical calculation shows indeed that oxygen adsorption at the step causes an outward relaxation of the surface layer and an expansion of the (100) nanofacet [22]. Indeed we find experimentally that the angular dependence of the 56 meV peak becomes less structured at higher coverage because the barrier for incorporation becomes so low that even molecules impinging along an unfavorable direction can overcome it thermally and access the subsurface site. An expansion of the outermost interlayer spacing after oxygen adsorption was reported also for other systems; e.g., for Ni(100)$c(2 \times 2)$O a 5% expansion takes place to be compared with a 3% contraction of clean Ni(100) [23]. O_{octa} may, however, be the final destination of part of the oxygen atoms after the crystal is annealed at or above room temperature. Finally, no significant occupation of the tetrahedral subsurface site occurs for O/Ag(410), since no loss around 56 meV is observed. This result might be indicative of a smaller relaxation of the Ag-O rows for O/Ag(410), so that access to subsurface sites is less favored.

In conclusion, we have shown that total oxygen dissociation occurs on Ag(210) already at $T = 105$ K and that different adsorption sites are present, characterized by different $\hbar\omega$. In particular, we observe the population of a metastable subsurface site, which can be accessed only in the presence of preadsorbed oxygen. It can be reached by oxygen adatoms by thermally overcoming an activation barrier at $T > 130$ K or by dissociating O_2 at $T = 105$ K. In the latter case, we observe a direct pathway, for molecules hitting the active site normally to the (100) nanofacets, and an indirect pathway, for molecules hitting the surface elsewhere or in the wrong direction, undergoing chemisorption and diffusing to the active site. We expect these results to be of general importance for all reactions for which one of the reactants moves to subsurface sites or plays a role in activating other adsorbed species.

We thank MIUR for financial support under PRIN 2001023192, T. Kokalj for making available unpublished calculations, and G. Rovida for providing the sample.

*Present address: Fachbereich Physik der Freien Universität Berlin Institut für Experimentalphysik, Arnimalee 14, D14195 Berlin, Germany.

[1] G. Ertl, Adv. Catal. **45**, 1 (2000).
[2] R. A. Van Santen and H. C. P. Kuipers, Adv. Catal. **35**, 256 (1990).
[3] C. T. Campbell and M. Paffett, Surf. Sci. **139**, 396 (1984).
[4] P. J. Van den Hoek, E. J. Baerends, and R. A. Van Santen, J. Phys. Chem. **93**, 6469 (1989).
[5] C. T. Campbell, Surf. Sci. **157**, 43 (1985).
[6] C. Backx, C. P. M. de Groot, and P. Biloen, Surf. Sci. **104**, 300 (1981).
[7] E. L. Garfunkel *et al.*, Surf. Sci. **164**, 511 (1985).
[8] L. Vattuone *et al.*, J. Chem. Phys. **115**, 3346 (2001).
[9] L. Savio, L.Vattuone, and M. Rocca, Phys. Rev. Lett. **87**, 276101 (2001).
[10] L. Vattuone *et al.*, Phys. Rev. Lett. **72**, 510 (1994).
[11] F. Buatier *et al.*, J. Chem. Phys. **106**, 9297 (1997).
[12] F. Buatier *et al.*, Chem. Phys. Lett. **270**, 345 (1999).
[13] G. Benedek *et al.*, Europhys. Lett. **53**, 544 (2001).
[14] A. D. Johnson, S. P. Daley, A. L. Utz, and S. T. Ceyer, Science **257**, 223 (1992).
[15] V. I. Bukthyarov *et al.*, J. Catal. **150**, 268 (1994).
[16] L. Savio *et al.*, Surf. Sci. **506**, 213 (2002).
[17] M. Rocca *et al.*, Rev. Sci. Instrum. **62**, 2171 (1991).
[18] R. D. Ramsier *et al.*, J. Chem. Phys. **100**, 6837 (1994).
[19] A. D. Johnson *et al.*, Phys. Rev. Lett. **67**, 927 (1991).
[20] C. M. Kim *et al.*, Surf. Sci. **327**, 81 (1995).
[21] L. Vattuone *et al.*, J. Chem. Phys. **109**, 2490 (1998).
[22] T. Kokalj *et al.* (unpublished).
[23] J. W. M. Frenken, J. F. Van der Veen, and G. Allan, Phys. Rev. Lett. **51**, 1876 (1983).